Journal of Membrane Science 714 (2025) 123408

Contents lists available at ScienceDirect

Journal of Membrane Science

journal homepage: www.elsevier.com/locate/memsci

Challenges of forward osmosis desalination processes using hydrogels as draw agents

Seyed Abdollatif Hashemifard [a,**], Mohammad Ali Ghanavatyan [a], Amir Jangizehi [b], Hasan Salehi [c], Alireza Shakeri [c], Qusay F. Alsalhy [d], Dhiyaa Al-Timimi [d], Christoph Bantz [b], Michael Maskos [b], Sebastian Seiffert [b,*]

[a] Sustainable Membrane Technology Research Group (SMTRG), Water research institute (WRI), Faculty of Petroleum, Gas and Petrochemical Engineering (FPGPE), Persian Gulf University, P.O. Box 75169-13798, Bushehr, Iran
[b] Department of Chemistry, Johannes Gutenberg University Mainz, Duesbergweg 10–14, D-55128, Mainz, Germany
[c] School of Chemistry, College of Science, University of Tehran, P.O. Box 14155-6619, Tehran, 141556455, Iran
[d] Membrane Technology Research Unit, Chemical Engineering Department, University of Technology-Iraq, Alsinaa Street 52, 10066, Baghdad, Iraq

ARTICLE INFO

Keywords:
Forward osmosis desalination
Hydrogels
Draw agents
Concentration polarization

ABSTRACT

The present study aims to investigate the properties, identification, and comprehension of the obstacles encountered in the forward osmosis process when utilizing a hydrogel drawing agent (FO-HG). Furthermore, a comparison is made between the FO-HG system and conventional forward osmosis systems employing a salt solution drawing agent. The comparison and evaluation of the swelling process of hydrogel and the kinetics of water penetration are conducted in both un-constrained and constrained states. Furthermore, the investigation and analysis are carried out to determine the presence or absence of internal concentration polarization (ICP) and external concentration polarization (ECP) phenomena. These phenomena are studied in situations with and without mixing, as well as in different orientations of the membrane (FO-mode and PRO-mode). The impact of these phenomena on the water flux of the systems FO-HG and FO-NaCl is also examined. An evaluation is conducted to determine the influence of the amount and size of hydrogel used as a draw agent in the FO-HG system on the water flux. The results of the study reveal that smaller hydrogel particles in the FO-HG system exhibit a higher flux compared to larger particles. Additionally, it is observed that the water flux in PRO-mode is unexpectedly higher when salt water is used as feed solution. This phenomenon can be ascribed to a counter-osmotic effect, originating from the FO state. Despite the high water absorption capacity of hydrogel and its potential as an ideal drawing agent in the forward osmosis process, the results demonstrate that the flux of the FO-HG system is inferior to that of the FO-NaCl system. Finally, the focus is on resolving the low flux issue by suggesting a process involving multiple cycles throughout day and night. We investigate the influence of hydrogel particle size, membrane surface, hydrogel layer thickness, as well as swelling and deswelling time in one cycle. The swelling time displays a peak at an optimal absorption duration, while the deswelling time does not show a similar optimal point, highlighting the difference between swelling and deswelling phenomena. Therefore, the hydrogels' high absorption capacity alone is insufficient for achieving desalination success. The research findings emphasize the high importance of synthesis of a membrane with minimal resistance, enabling a high water flux and suitable selectivity.

1. Introduction

The exponential increase in the global population, accompanied by gradual expansion of industrial activities, climate change, and scarcity of fresh water resources, has transformed the provision of drinking water for daily use and the water required by industries into a significant challenge [1–4]. Various solutions have been proposed to address this challenge, including the desalination of sea water and brackish waters as well as the treatment of wastewater [5–7]. Membrane technology has emerged as a key technology in water and wastewater treatment

* Corresponding author.
** Corresponding author.
E-mail addresses: salhashemifard@pgu.ac.ir (S.A. Hashemifard), sebastian.seiffert@uni-mainz.de (S. Seiffert).

https://doi.org/10.1016/j.memsci.2024.123408
Received 9 August 2024; Received in revised form 4 October 2024; Accepted 13 October 2024
Available online 15 October 2024

processes, primarily due to its efficient removal of pollutants from water sources [8]. Nevertheless, membrane processes such as reverse osmosis and nanofiltration entail substantial operating costs due to the necessity of hydraulic pressure to counterbalance the osmotic pressure of the feed water. Thus, the forward osmosis (FO) process is presently being deemed as a suitable candidate and alternative for the mentioned processes [9–11].

The forward osmosis (FO) process involves the utilization of a semi-permeable membrane and two solutions, namely a feed solution (FS) and draw solution (DS), which possess distinct osmotic pressures. This difference in osmotic pressure is the driving force in FO processes for water transport between the feed solution (with low osmotic pressure) and the draw solution (with high osmotic pressure), while the semi-permeable membrane effectively hinders the movement of ions [12–17]. Unlike the RO process, the FO process does not require significant hydraulic pressure [18]. The choice of a suitable draw agent should take into account factors such as chemical stability and compatibility with the FO membrane [12,17,19–21]. The perfect forward osmosis membrane should possess an active layer that exhibits suitable selectivity and a substrate that allows for high flux. Additionally, its structure should be designed in a manner that minimizes concentration polarization, reverse salt flux (RSF), and fouling. The FO processes often face several challenges, including high reverse salt flux, concentration polarization (both internal and external), low mechanical strength of the membrane, limited flux, and substantial energy consumption for regenerating the draw solution and recovering water from the draw solution [5]. Factors like solute properties, membrane surface properties, membrane structure, and hydrodynamics play a crucial role in controlling concentration polarization [22–24]. In FO processes, the reverse solute flux arises from the variation in solute concentration between the two sides of the membrane. Consequently, the reverse salt flux diminishes the effective osmotic pressure difference between the two sides of the membrane, resulting in a decrease in the efficiency of FO systems [25–27].

In recent years, hydrogels have gained significant attention as draw agents in the FO process due to their distinct properties [28,29]. Hydrogels are generally polymer based materials that are formed through inter-chain physical or chemical crosslinking, resulting in the development of a three-dimensional network structure. Typically, hydrogels have the ability to absorb water several times compared to their own dried weight [30–35]. Researchers were convinced to utilize hydrogels as the draw solution in the FO process due to their ability to exert substantial osmotic pressure and achieving a dramatic swelling ratio. The recovery and regeneration of these entities can be facilitated through external stimuli such as temperature, pressure, and pH, thereby creating an opportunity in this field. Furthermore, the fact that they are not soluble in water appears to prevent the occurrence of reverse solute flux during the forward osmosis procedure.

The hydrogel plays a crucial role in a FO-HG system. The driving force and performance of the FO-HG system are significantly influenced by various factors, including the chemical structures, cross-linking density, and particle sizes of pure hydrogels [28]. Li et al. [36] conducted the initial exploration into the capabilities of ionic and non-ionic hydrogels as novel type draw agent for forward osmosis. Through their analysis of the impact of charge density on the swelling pressure of these hydrogels, they determined that ionic hydrogels exhibit greater water flux in comparison to non-ionic hydrogels. They showed that their hydrogels exhibited an initial water flux ranging from 0.1 to 1.1 LMH during the forward osmosis process when deionized water was used as the feed solution. This flux is notably lower when compared to other draw solutions that contain inorganic salts. For instance, a draw solution of 0.5 M NaCl resulted in a flux of 20.5 LMH when 10 mM NaCl was utilized as the feed solution [37]. Additionally, the water flux was reported to be 1–3.57 LMH for a draw solution of CuSO4 (0.5–1.0 M) with brackish water as the feed solution [38], and 7.55–15.1 LMH for a draw solution of MgCl2 (1.7–6.9 g/L) with 33 mg/L NaCl as the feed solution [39]. The impact of hydrogel particle size on water flux has been highlighted by Omidian et al. [40]. Smaller particles exhibited a higher surface-to-volume ratio, resulting in a greater contact surface area and subsequently a higher water flux. Razmjoo et al. [41] identified larger surface area, greater interstitial volume, and narrower capillary pores as the contributing factors to the higher osmotic pressure observed in smaller hydrogel particles. An essential attribute of hydrogels is their low reverse diffusion rate, which is a result of their insolubility in water [42]. Ma et al. [43] conducted a study on the impact of various draw solutions on the internal and external concentration polarizations, as well as their influence on the effective osmotic pressure in the FO process, based on the model and experimental data. This research revealed that an increase in the concentration of the draw solution, in the absence of CP limitations, leads to a higher osmotic pressure and subsequently, a greater water flux. In contrast, Wang and et al. [44] asserted that the osmotic pressure is diminished by CP effects, causing a decrease in water flux. This suggests that CP effects have counteracted a substantial amount of the osmotic pressure driving force. Hence, with the increase in draw solution concentration, the influence of CP becomes more pronounced. The decline in water flux due to both ECP and ICP effects is significantly more substantial than the decrease in water flux resulting from ECP alone, indicating that ICP is the predominant limitation on water flux performance in the FO system [43].

Despite these important achievements, researchers faced important obstacles such as concentration polarization, low water flux, and process discontinuity, as highlighted in a series of studies [36,42,45–47]. The main goal of this study is to investigate, recognize, and enhance comprehension of the challenges posed by the FO-HG system in comparison to conventional FO systems that utilize salt solutions as the drawing agent. In this research, sodium acrylate hydrogels are utilized as the drawing agent in the FO-HG process. The FO-HG process is carried out under two conditions, with and without mixing of the feed solution, to evaluate and explore the impact of internal and external concentration polarization on the water flux. Furthermore, the obtained results are analyzed and reviewed by considering the resistance relationships in the FO-HG system in different membrane directions (FO and PRO-mode). This study introduces an innovative approach by examining the concentration or osmotic pressure profile as a driving force for fresh water flux in FO-HG systems. It includes a comparative analysis of hydrogel versus non-hydrogel draw solutions within forward osmosis systems (which are hereafter referred to as FO-NACL and FO-HG systems, respectively), thereby addressing the challenges associated with the FO-HG system. To gain insights into the phenomenon of water diffusion into hydrogel and its kinetics, the swelling behavior of the hydrogel is assessed in both un-constrained and constrained states. Furthermore, the attention is directed towards addressing the low flux problem, therefore a multicyclic system is proposed as an alternative to a batch system to optimize the fresh water flux. Additionally, the impact of operational parameters on the performance of the proposed continuous FO-HG system has been thoroughly investigated. The research delves into examining the impact of hydrogel particle size, membrane surface, hydrogel layer thickness, along with swelling and deswelling time within a multicyclic process. We emphasis that the type of membrane is not the focus of this study; whether it is an RO membrane or a specific FO membrane, both can fulfill the objectives of our research. Ongoing work within our research group is dedicated to identifying a suitable membrane for the FO-HG application.

2. Experimental

2.1. Materials

In both the FO-NaCl and FO-HG systems, the TW30-1812-75HR model of the RO Film-Tec commercial membrane, manufactured by DUPONT, served as the semi-permeable membrane for the forward osmosis process. In the FO-HG system, TAISAP BC 283FA sodium

acrylate superabsorbent were employed as the drawing agent. On the other hand, in the FO-NaCl system, draw solutions and feed solutions with different concentrations of NaCl salt, manufactured by Merck (99.5 %) in Germany, were utilized.

2.2. Measurements and tests

2.2.1. Flux measurement in FO-HG system

In the FO-HG system as shown in Fig. 1, a glass setup was utilized which consists of two separate cylindrical parts. The membrane between these two cylindrical parts was held in place by a flange. 1.5 g of superabsorbent as a drawing agent was placed on the upper side of the membrane, while on the opposite side of the membrane, the desired concentration feed solution was introduced from within the burette connected to the lower part of the glass setup. A plastic cap was utilized to cover the upper end of the system to prevent the hydrogen from evaporating during the course of the experiment. By changing the orientation of the membrane, the FO-mode (the active layer facing the feed solution) and the PRO-mode (the active layer facing the draw agent) were evaluated. The feed solution concentration underwent changes in different trials, from pure water to NaCl salt solutions with concentrations of 2000, 10000, and 30000 mg/L. The membrane's effective area, which referred to the surface of the membrane in contact with the feed solution, measures 19.6 cm^2. To determine the volume of water absorbed by the hydrogel, reduction of the volume of the feed solution in the burette at 2-h intervals over a period of 24 h was considered. By utilizing Eq. (1) [48], the water flux; J (LMH) in various modes within the FO-HG system was then calculated.

$$J = \frac{V}{A \times t} \tag{1}$$

In this equation, V (L) is the volume of the adsorbed water by hydrogel, A (m^2) is the effective surface area of the membrane, and t (h) is duration of water absorption in each step.

2.2.2. Flux measurement in FO-NaCl system

Referring to Fig. 1, in the FO-NaCl system, a drawing agent composed of 8 g of 0.25 M, 0.5 M and 1.0 M NaCl salt solution was utilized in both FO and PRO modes, without any agitation. The feed solution encompassed NaCl solutions with different concentrations (2000, 10000, and 30000 mg/L), alongside pure water. The recorded data in this section pertains to the reduction in volume of the desired feed solution compared to a specific amount at the start of the process in the burette, measured at regular time intervals, and Eq. (1) was utilized to calculate the water flux.

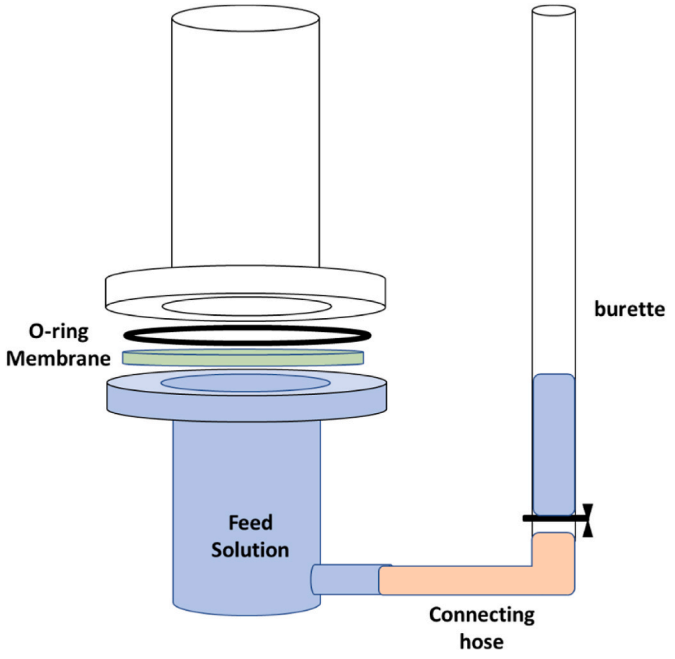

Fig. 1. Forward osmosis system setup.

2.2.3. Concentration polarization (CP) measurement test

The forward osmosis process was carried out in both FO and PRO modes within the FO-HG system. The feed solution encompassed various compositions, including pure water and NaCl salt solution with concentrations of 2000, 10000, and 30000 mg/L. Two different conditions were employed during the testing process, i.e. agitation and no-agitation of the feed solution to examine the occurrences of internal concentration polarization (ICP) and external concentration polarization (ECP). In this experiment, a magnet stirrer was used to effectively control the ECP in the FO and PRO processes. By creating turbulency, the presence or absence of ICP and ECP phenomena in each state could be determined, depending on the orientation of the membrane. Furthermore, the assessment of their influence on water flux was carried out in both FO and PRO modes.

2.2.4. Measurement of hydrogel swelling in un-constrained and constrained states

The investigation focused on the swelling ratio of the hydrogel in the un-constrained state, when it came into contact with water from all sides. A tea bag, containing 0.05 g of hydrogel, was used to immerse the hydrogel in pure water and NaCl salt solutions at concentrations of 5000, 10000, 20,000, and 30,000 mg/L. The experiment lasted for a duration of 80 min. To investigate the swelling of the hydrogel in a constrained state, where it was not in contact with water from all sides but only on one side, a piece of fabric was employed as a substitute instead of membrane in the FO setup. The fabric served solely as a means to hold the hydrogel in place within the experimental setup depicted in Fig. 1. The size of the fabric pores was sufficiently large that the resistance against water diffusion in the HG could be easily disregarded. The hydrogel absorbed pure water as a feed solution by allowing it to pass through the fabric. Since the fabric offered minimal resistance to water penetration from the feed side to the hydrogel side, it was crucial to maintain consistent conditions and prevent a sudden decrease in the height of the pure feed water inside the burette. To achieve this, the volume of feed inside the burette was regularly monitored and recorded over a period of 80 min, in between any decrease immediately compensated by adding pure water to maintain the initial level. This ensured that no hydraulic pressure difference occurred and the experiments proceeded with minimum error. The hydrogel's swelling ratio (SR) was derived by employing Eq. (2) [49].

$$SR = \frac{W_S - W_d}{W_d} \tag{2}$$

Where W_d, and W_S denote mass of the dry hydrogel, and swollen hydrogel at a given time, respectively.

2.2.5. Investigating the effect of hydrogel mass and particle size on FO-HG system

To evaluate how hydrogel mass impacts water flux in the FO-HG system, two different quantities of hydrogel, 1.5 and 0.5 g, were utilized as the drawing agent in the FO-mode using pure water as the feed solution. The investigation and analysis of hydrogel thickness can also be conducted through this test. The evaluation of hydrogel particle size as a draw agent in the FO-HG system was performed using various hydrogel sizes of equal mass. Dry hydrogels were produced at the desired micro scale by employing the NARYA-MPM-2*250H planetary ball-mill, manufactured in Iran, operating at a speed of 350 rpm. The ratio of 10:1 (weight of balls to weight of dry hydrogel) was maintained

throughout the milling process, which lasted for a duration of 4 h. The measurement of hydrogel particle size distribution was conducted using Image Processing and Analysis in Java 8 (Image J) software. Initially, photographs of hydrogel particles in three different sizes were captured on a designated surface. These photographs were then calibrated using a specific scale. By utilizing the particle size distribution feature of the Image J software, the surface area and abundance of hydrogel particles in the captured images were determined. Subsequently, based on the acquired area and abundance data, graphs illustrating the distribution of hydrogel particle sizes were plotted, depicting the relationship between the hydrogel particle radius in micrometers and their abundance in all three cases.

3. Results and discussion

3.1. Effect of salt concentration on hydrogel equilibrium swelling

The correlation between time and the amount of equilibrium swelling of the hydrogel is presented in Fig. 2. The data was collected through the tea bag test, where the hydrogel was immersed in containers with varying concentrations of the feed solution. When the solution contained NaCl salt with increasing concentrations, the osmotic pressure of the solution also increased, leading to a decrease in the osmotic pressure difference between the solution and the hydrogel. As a result, the hydrogel equilibrium swelling experienced a decreasing trend as the salt concentration increased. It should be noted that a significant reduction in the swelling ratio occurred at extremely low levels of NaCl concentration, specifically below 1000 mg/L. According to Li et al., the equilibrium swelling rate decreased with increasing the ionic strength (which is an indicative of the salt concentration) of the solution [50].

3.2. Effect of different feed concentrations on FO-HG system performance

The changes in flux of the FO process in the FO-HG system as a function of time are depicted in Fig. 3. The study examined the behavior of both pure water and NaCl solution with different concentrations as the feed solution over time. The investigation was carried out in two modes, FO and PRO, without stirring of the feed solution. Based on the data presented, it is evident that the water flux has consistently decreased over time in both FO and PRO modes. It is noteworthy that the highest water flux was observed when pure water was utilized as the feed in both FO and PRO modes. The flux decreased due to a reduction in the osmotic pressure difference across the membrane. The presence of pure water as a feed solution eliminated the challenge of ICP and ECP due to the absence of solutes. Conversely, when a NaCl solution with different concentrations was employed as the feed in the FO-HG system, as water permeated from the feed solution to the hydrogel, the feed solutes accumulated near the surface of the active layer, leading to the

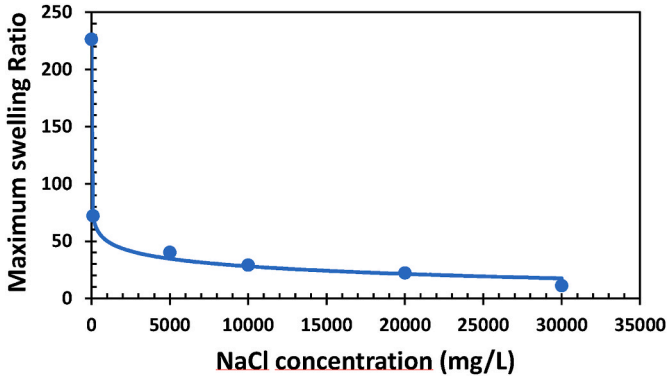

Fig. 2. Swelling of hydrogel in different feed concentrations in unconstrained state.

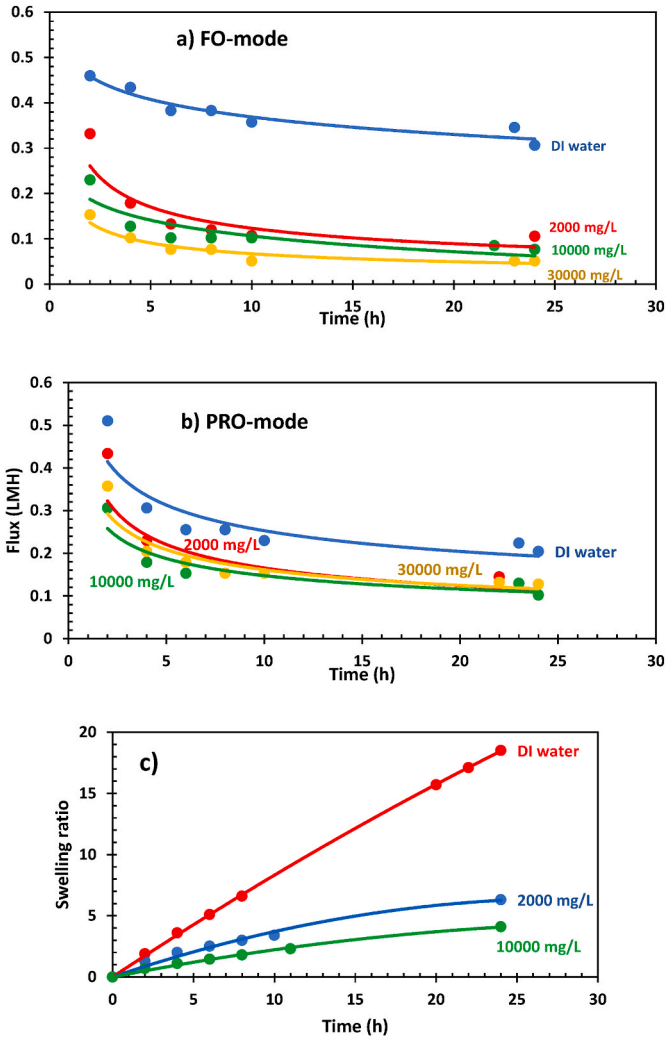

Fig. 3. Water flux against time for different concentrations of feed solution in two cases: a) FO-mode, b) PRO-mode. c) Comparison of swelling ratio in different concentrations of feed in the FO-HG system.

activation of the ECP phenomenon on the selective layer and a decrease in the osmotic pressure difference [36]. On the other hand in the FO-mode, due to the presence of hydrogel and its insoluble property, the substrate contains only pure water, thus ICP is prevented. In PRO-mode, as the feed solutes permeate the substrate's pores, in conjunction with ECP, ICP arises in the substrate. It should be emphasized that the hydrogel's water absorption takes place through molecular penetration, resulting in a strong ECP of the dilution type within the hydrogel in both FO and PRO modes. Obviously, also the utilization of pure water as feed results in a decrease in flux over time. This decrease in flux leads to a reduction in both the osmotic and swelling pressure of the hydrogel, consequently causing a decrease in the driving force. Furthermore, it can be observed from Fig. 3a and b that the flux curves for feeds containing different salt concentrations in the PRO-mode exhibited a closer resemblance to each other compared to the FO-mode. This indicates that in the PRO-mode, ICP is controlling the system which is almost the same for all feed concentrations. But in FO-mode, there is no ICP and the differences are due to the ECP difference.

The variation in the degree of swelling of the hydrogel as a function of time is visualized in Fig. 3c, providing insights into the influence of different concentrations of the feed solution during the forward osmosis test. Based on Fig. 3c, it is evident that over time, water permeates from the feed solution side and through the membrane. Consequently, the hydrogel absorbs the water, leading to a gradual swelling of the

hydrogel (as shown in Fig. S1). Notably, the rate of swelling and water absorption exhibits a steeper slope during the initial hours of the process compared to the later stages. The water absorption capacity of hydrogel is reliant on its swelling pressure. With an increase in water absorption, the swelling pressure of hydrogel gradually decreased, leading to a decrease in water flux. Fig. 3a and b clearly depict the gradual decrease in flux over time in both FO and PRO modes, regardless of the concentration of the feed solution. When pure water was employed as the feed in the process, the highest degree of flux and swelling was observed. This can be attributed to the notable discrepancy in osmotic pressure between pure water and hydrogel, which exceeded the difference in osmotic pressure between NaCl salt solutions and hydrogel. As a result, a more pronounced driving force was established. Additionally, the use of pure water as feed led to a higher water absorption rate by the hydrogel during the early hours of the process. In contrast, when the feed contained NaCl salt with different concentrations was used, as the concentration of NaCl feed solution became higher, the osmotic pressure of the feed solution increased, leading to a decrease in the osmotic pressure difference across the membrane and a subsequent reduction in the driving force of the process. In this case, the hydrogel absorbed water at a comparatively slower rate, resulting in a lower percentage of swelling. Consequently, leading to a gradual swelling process and a delayed attainment of equilibrium swelling.

3.3. Effect of ECP and ICP and air bubble entrapment

Fig. 4 illustrates the contrast in flux between FO-mode and PRO-mode under two distinct conditions: with and without using stirrer in the feed side. The experiment was conducted using two different concentrations of NaCl solution as feed (10000 and 30000 mg/L) in the FO-HG system. Agitation resulted in a significantly higher flux compared to the flux obtained without agitation in both scenarios. This can be attributed to the effective control of ECP through the generation of a turbulent flow in the feed solution, which subsequently reduced the resistance of the feed side boundary layer. As previously discussed, the decrease in flux can be attributed to the reduction of the osmotic pressure difference. This reduction was caused by concentration polarization on both sides of the membrane (both the NaCl feed solution side and the HG side), which was in turn achieved by increasing the salt concentration in the feed for both FO and PRO modes and swelling the HG. As stated earlier, even in the absence of concentration polarization in the feed solution, the swelling of the hydrogel leads to a decrease in the difference of osmotic pressure due to the reduction in charge density between the hydrogel and feed solution. This decrease ultimately leads to a decrease in the water flux. The presence of concentration polarization aids to highlight this reduction.

Based on the data presented in Fig. 4c, it can be observed that the flux in FO-mode is greater than the flux in PRO-mode when using pure water as the feed. The experimental setup involved a horizontal membrane, which was initially dry, with an air-filled substrate. It is possible that the presence of air bubbles trapped under the active layer in PRO-mode created a resistance, resulting in a lower flux compared to FO-mode. The comprehension of this can be achieved by focusing on Fig. S2a. Figs. S2b and S2c depict the membrane in FO and PRO modes respectively, right after coming into contact with water, without any delay. The observation of the upper surface of the membrane reveals wetting in FO-mode, accompanied by a transient air bubble that quickly disappears; this phenomenon is absent in PRO-mode. Nevertheless, after a duration of 1.5 h, the surface of the membrane in PRO mode (Fig. S2d) exhibited wetting as the entrapped air was progressively expelled, although a few air bubbles remained (as shown via dotted red circle). These observations provide confirmation for the stated hypothesis. Accordingly, in PRO-mode, the hydrogel's water absorption time can be prolonged not only by the resistance of the membrane but also by the resistance caused by trapped air, resulting in a decrease in flux. This phenomenon has not been documented in the existing literature

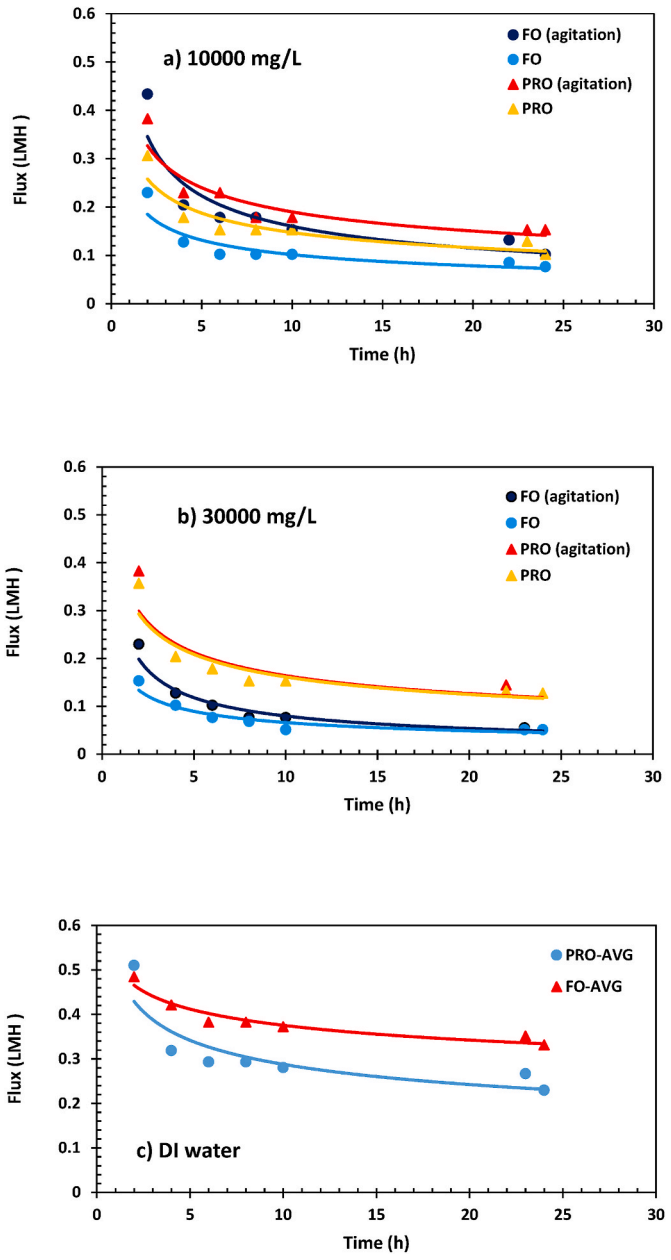

Fig. 4. FO and PRO flux diagrams in the FO-HG system in two situations with stirrer and without stirrer in NaCl feed solution with concentrations of a) 10000 mg/L, b) 30000 mg/L, c) pure water.

concerning FO-HG systems.

The statement commonly made is that generally the water flux is greater in PRO mode compared to FO mode. However, this assertion holds true solely for traditional FO systems when the feed consists of pure water, thereby eliminating ICP from the feed side. In the case of real feed solutions e.g. wastewater feeds the FO-mode and PRO-mode fluxes can be comparable. Particularly for the FO-HG system in FO mode, since there is no ICP on the HG side and due to the presence of ICP in the feed side, it is anticipated that the flux in PRO-mode would be lower than in FO-mode. However, the data presented in Fig. 4a and b exhibit a contradictory scenario. Specifically, the flux in PRO-mode for salt water feed outperforms that of FO-mode. The change in behavior observed between salt water feed and pure water feed prompts the query: what is the cause behind it? (Refer to Fig. 4a, b, 4c). The potential explanation for this matter could lie in a counter-osmotic effect (Fig. 5a). Due to water penetration and passage through the active layer in FO-

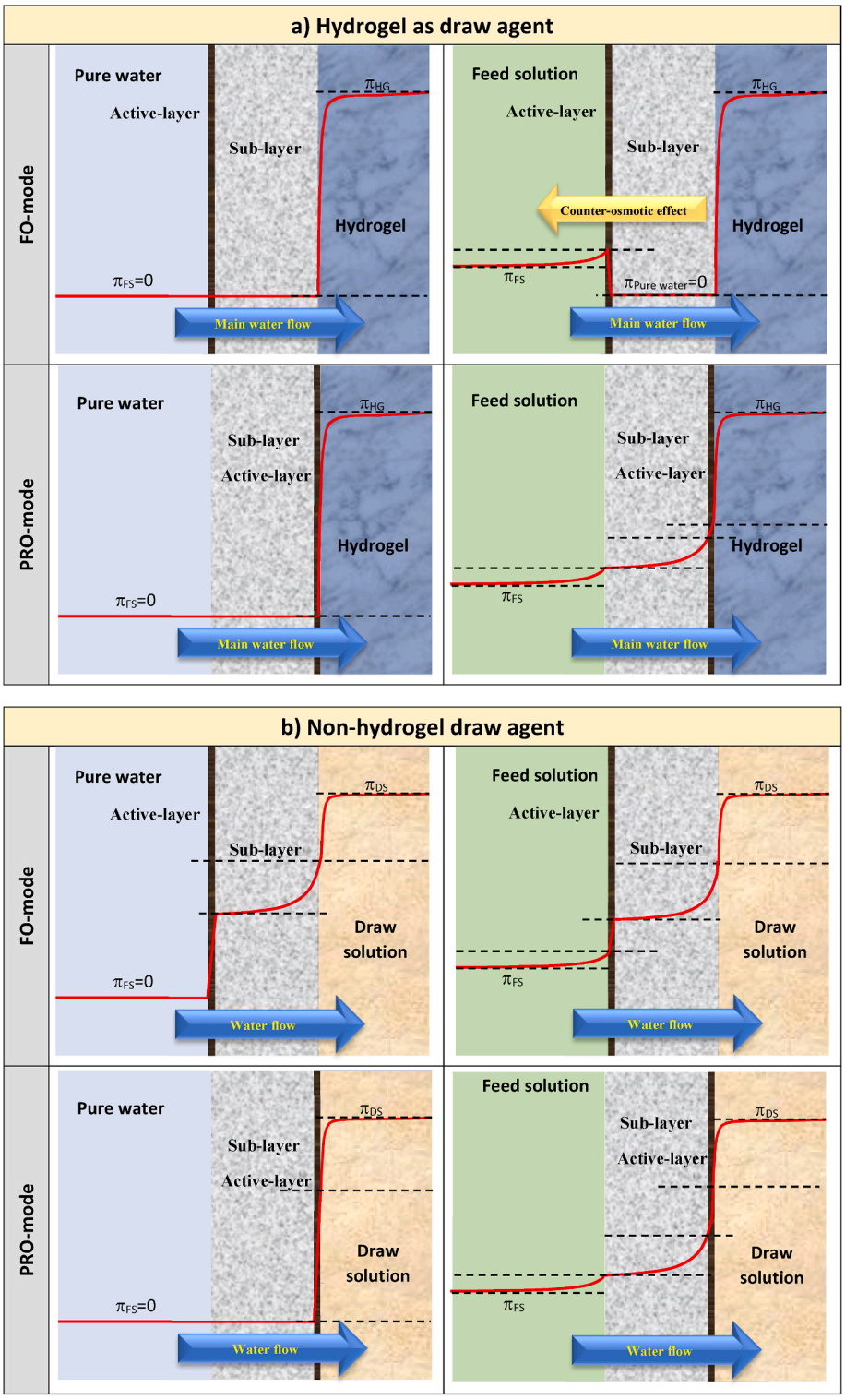

Fig. 5. Schematic description of osmotic pressure profile in a) FO-HG system and b) FO-Non-HG system for FO and PRO modes.

mode, pure water accumulates in the substrate. This accumulation creates an osmotic pressure difference between the pure water in the substrate and the feed water, resulting in a reverse osmotic flux from the substrate side to the feed side. The decrease in the net flux of the system is likely attributed to this factor. Analyzing the resistances of both scenarios can provide valuable insights. Referring to Fig. 5 for the FO-mode, the total resistance can be written as:

$$R_t^{FO} = R_{ECP}^{FO} + R_{AL}^{FO} + R_{COE}^{FO} + R_{ICP}^{FO} + R_{SL}^{FO} + R_{air}^{FO} + R_{IF}^{FO} + R_{HG}^{FO} \quad (3)$$

and for PRO-mode:

$$R_t^{PRO} = R_{ECP}^{PRO} + R_{ICP}^{PRO} + R_{SL}^{PRO} + R_{air}^{PRO} + R_{AL}^{PRO} + R_{IF}^{PRO} + R_{HG}^{PRO} \quad (4)$$

Considering the non-ideal contact between HG and the membrane surface, an interfacial resistance R_{IF} is factored in for both modes. The experimental results of the flux indicate that the overall resistance in the FO-mode is higher than that of the PRO-mode:

$$R_t^{FO} > R_t^{PRO} \quad (5)$$

$$R_{ECP}^{FO} + R_{AL}^{FO} + R_{COE}^{FO} + R_{ICP}^{FO} + R_{SL}^{FO} + R_{air}^{FO} + R_{IF}^{FO} + R_{HG}^{FO} > R_{ECP}^{PRO} + R_{ICP}^{PRO} + R_{SL}^{PRO} + R_{air}^{PRO} + R_{AL}^{PRO} + R_{IF}^{PRO} + R_{HG}^{PRO} \quad (6)$$

Upon comparing the resistances of the two modes, it becomes evident that the overall resistance of the FO-mode is greater than that of the PRO-mode. Specifically, this higher resistance is attributed to the counter-osmotic effect, denoted as R_{COE}^{FO}. The agitation effectively regulates the resistance of ECP, known as R_{ECP}. The resistance of the active layer of the membrane (R_{AL}) is nearly identical for both modes. The substrate resistance due to the structure (R_{SL}) remains consistent for both modes. The ICP resistance is insignificant in the FO-mode compared to the PRO-mode, assuming that the hydrogel does not release ions. The resistance caused by HG, denoted as R_{HG}, is approximately the same for both modes. After simplifying Eq. (6), the equation can be rewritten as follows:

$$R_{COE}^{FO} > R_{ICP}^{PRO} + R_{air}^{PRO} \quad (7)$$

Based on this analysis, it can be concluded that the counter-osmotic effect in FO-mode exerts a stronger influence compared with the resistance of ICP (R_{ICP}) along with the resistance of air bubbles (R_{air}) within the substrate in PRO-mode. Consequently, the flux in PRO-mode is higher than that in FO-mode. It is important to highlight that in cases where the fouling effects are severe from the ICP type, e.g. real wastewater the superiority of FO-mode over PRO-mode should be considered and studied. Fig. 5 further demonstrates a conceptual contrast between FO-HG system and FO systems using non-hydrogel draw agent by showcasing the osmotic pressure profile across various sections of the system. However, there are similarities in the osmotic pressure profile in these two systems. For instance, when the feed consists of pure water, the profile remains almost identical regardless of the membrane configuration in the feed side. It is evident that in the case of FO-HG, as opposed to FO-non-HG, reducing the ECP in the hydrogel is not feasible. Also, in PRO-mode with real feed solution, similarities can be observed in their profiles. However, the most significant contrast arises when comparing FO-mode with a unique real feed solution. In such instances, the osmotic pressure profile in the substrate significantly differs between FO-HG and FO-non-HG. The underlying cause appears to be the counter-osmotic effect. In FO-HG mode, the ICP resistance is almost nonexistent, whereas in FO-non-HG mode, the ICP resistance is fully present and impactful.

3.4. Effect of different feed concentrations on water flux in FO-NaCl system

Figs. S3a–S3d illustrates the water flux diagrams in FO and PRO modes, showcasing various feed solutions within the FO-NaCl system without stirring. Based on Figs. S3a and S3b, as usual there was a declining trend in the water flux for feed concentrations of 2000, 10,000 and 30,000 mg/L in both FO and PRO modes. The concentration of the feed or draw solution played a significant role in determining the resistance caused by ECP and ICP in either side. This resistance most likely reached a critical value and a certain limit. When the concentration exceeded this critical limit, the effectiveness of concentration polarizations decreased. Consequently, the flux values at high concentrations (e.g. 10000 and 30000 mg/L) became similar with only a slight difference, as depicted in the Figures. The observation of the same phenomenon in the case of FO-HG was illustrated by Fig. 3a and b.

In both FO and PRO modes, the water flux was naturally at its highest when the feed solution consisted of pure water (Figs. S3a and S3b). According to the results, the use of pure water as feed in PRO-mode led to a higher flux compared to FO-mode. This disparity can be explained by the fact that in PRO-mode, the substrate was located on the feed side. Furthermore, since the feed was composed of pure water, the ECP and ICP on the feed side did not exert any influence, and only the ECP on the draw solution side was observable. However, in FO-mode, the impact of both ECP and ICP was observed on the draw solution side. Water diffusion from the active layer of the membrane on the feed side caused the dilution of ICP and ECP, affecting the overall resistance. Simultaneously, the effect of ECP was nullified on the feed side, which solely comprised pure water. Therefore, the flux in PRO-mode was anticipated to be superior to FO, as evidenced by the findings of the experiments.

When using a salt solution feed in PRO-mode, the higher concentration of DS compared to FS leads to lower resistance on the feed side than on the draw solution side. Consequently, it is expected that the PRO-mode will have a higher flux than the FO-mode. However, certain factors may disrupt and alter the situation. For example, the presence of actual wastewater as a feed e.g. wastewater from food processing plants like dairy factories etc. or the entrapment of air bubbles in the substrate when the system is set up vertically, as illustrated in Fig. 1 and S2a. In cases where the feed solution is saltwater or actual wastewater, the air bubbles, due to the higher surface tension at higher concentrations compared to pure water [51], may become more deeply trapped in the substrate and may prove challenging to release from the skin layer. Consequently, it is observed that the flow rate in PRO-mode is lower than that in FO-mode under more realistic conditions, as indicated by the results of the experiments conducted in Fig. S3b. Therefore, in scenarios involving more realistic feed solutions, fouling, particularly irreversible fouling, can lead to a significant decrease in the PRO-mode flux. The selection of FO-mode or PRO-mode and its impact on the FO process in terms of flux behavior and membrane fouling has been extensively studied by various researchers. Tiraferri et al. [52] highlighted that operating the FO process in the PRO-mode can result in a higher water flux. This is because the draw solution is in direct contact with the active layer and is less affected by internal concentration polarization (ICP). However, when real wastewater is used as the feed solution, membrane fouling is more pronounced in the PRO-mode due to the contact between the support layer and the feed solution. Zhao et al. (2022) further explored [53] the feasibility of double-skinned forward osmosis membranes with improved flux and antifouling properties for sludge thickening. Additionally, Eyvaz et al. [54], Alihemati et al. [1] and Ansari et al. [55] provided a comprehensive review on forward osmosis membranes. Consequently, the FO-mode is widely employed in wastewater treatment applications. Fig. 3 and S3 reveal several significant points upon comparison:

1- In general, in the majority of cases within the FO-NaCl system, even with a draw solution concentration of 0.25 M, the water flux surpasses the FO-HG system. As the concentration of the draw solution decreases, leading to a reduction in the osmotic pressure difference in the FO-NaCl system, the flux experiences a significant decrease. This reduction is so pronounced that when the concentrations on both sides of the membrane are equal, the flux tends to zero. This phenomenon is illustrated in Fig. S3c for a draw solution concentration of 0.5 M with a feed concentration of 30,000 mg/L, and in Fig. S3d for a draw solution concentration of 0.25 M with a feed concentration of 10,000 mg/L. Unlike the FO-NaCl system, the flux in the FO-HG system did not decrease to zero at any of the feed concentrations of 0, 2000, 10000, and 30000 mg/L.

To enhance comprehension of the subject, Fig. S4 illustrates the variations in osmotic pressure difference between the draw solution and the feed solution across different feed concentrations, alongside the draw solution with varying concentrations and the hydrogel. The first water fluxes from Fig. 3a–S3b, S3c and S3d have been used as input in equation (8).

$$J = L_P(\pi_D - \pi_F) \quad (8)$$

In this equation, the term in the parentheses is the osmotic pressure difference (π_D and π_F are the draw and feed solution osmotic pressure respectively), and L_P is the water permeability which was measured as 1.9 LMH/bar for the used membrane. The data indicate that as the concentration of the draw solution decreases, both the osmotic pressure difference and the water flux approach zero. Under these circumstances,

the hydrogel tested maintains a nearly constant flux, which does not reach zero across all examined feed concentrations (0, 2000, 10000 and 30000 mg/L). It is important to note that theoretical calculations suggest that the osmotic pressure difference and water flux are significantly greater than the values observed in the laboratory, by one to two orders of magnitude, a reduction attributed to the effects of internal and external concentration polarization.

This highlights a significant conceptual distinction between the absorption mechanisms in hydrogel and salt water as a draw agent. In hydrogel, the driving force is the swelling pressure, whereas in salt water solution, it is the osmotic pressure. The experimental results showcased in Fig. 3 and S3 may serve as a practical resolution to the ongoing debate regarding the most suitable and logical term for water absorption in a hydrogel. This debate was sparked by the article authored by Zhao et al. [56] and Wang et al. [57]. The swelling pressure of an ionic polymer hydrogel can be divided into three components [58]: mixing, elastic, and osmotic phenomenon caused by the contribution of ions in the hydrogel. Therefore, osmotic pressure assigns a component of the swelling pressure to facilitate water absorption, and each component operates according to its own mechanism that their resultant manifests as the swelling pressure. In the FO-HG system, the non-zero flux indicates that, apart from the ion term, the mix and elastic terms are actively involved.

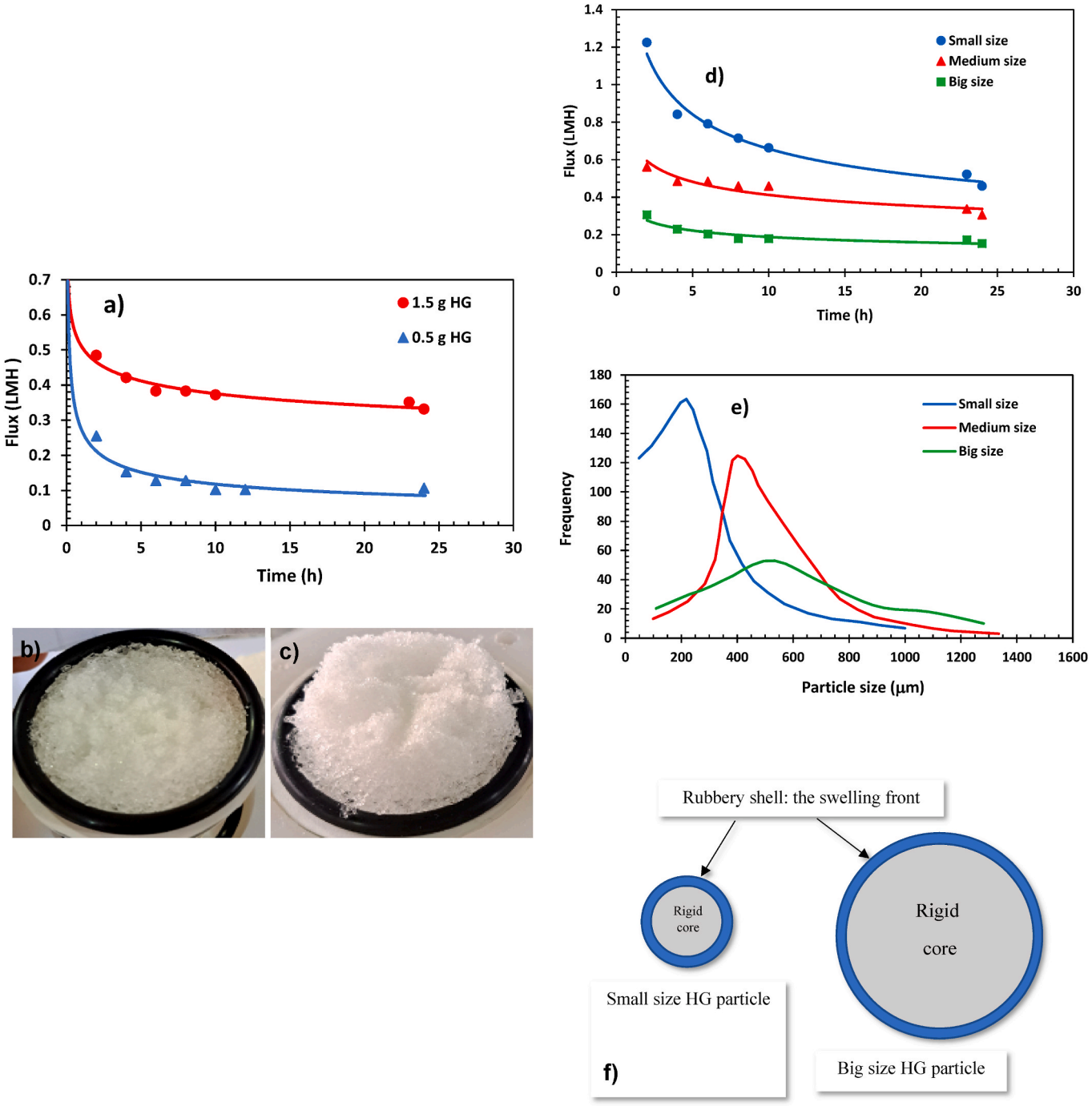

Fig. 6. Comparison of flux in FO-HG system with pure water feed in FO-mode during 24 h a) Effect of different amount of hydrogel on water flux, b) Swelling of 0.5 g of hydrogel after completion of the experiment, c) Swelling of 1.5 hydrogel after completing the experiment, d) the effect of hydrogel particle size on water flux, e) hydrogel particle size distribution, and f) schematic of a small an a big hydrogel particle during the swelling process.

On the other hand, in the FO-NaCl system, the flux tends towards zero due to the concentration tendency of saltwater on both sides towards each other. This is because only the ion concentration difference mechanism or the osmotic pressure mechanism acts as the driving force in this system.

2- The duration of the test for FO-HG in Fig. S3 spanned 24 h, whereas it only lasted for 4 h in the FO-NaCl system. If the test was prolonged for the FO-NaCl system, the flux would inevitably drop to zero quickly. On the other hand, in the FO-HG system, the flux did not reach zero even after 24 h, thanks to the unique swelling characteristic of HG, which exhibits a high water absorption capacity.

A further distinction between the two systems lies in their capacity to diminish ECP resistance on the draw solution side. This reduction is achievable in the FO-NaCl system through the high mobility of DS, which allows for turbulence generation. Conversely, in the FO-HG system, characterized by high viscoelasticity, such reduction is unattainable. The uncontrollable aspect of the ECP of the hydrogel as a draw agent is a direct result of the process's nature. Furthermore, within the FO-HG system, the FO-mode yields a draw agent side ICP value of zero. Conversely, in the FO-NaCl system, none of the modes produce an ICP value of zero. To sum up, a perfect equivalence between an FO-NaCl system and an FO-HG system is extremely difficult to establish, considering the reasons stated above. In order to replace the usual draw solutions by hydrogels, it is essential for the hydrogel to absorb a substantial amount of water during reaching the equilibrium. Additionally, the limited contact area between the hydrogel and the membrane gives rise to an augmented interstitial volume within the hydrogel-hydrogel particles and hydrogel-membrane interface. This augmentation subsequently diminishes the capillary force and water penetration, resulting in a decrease in the flux [40,41,59].

3.5. Effect of amount and size of hydrogel particles on FO flux

In the FO-HG system, the driving force is a result of the osmotic pressure discrepancy between the hydrogel particles and the feed solution on both sides of the membrane. Different masses of hydrogel were examined to determine their effect on osmotic pressure and the flux of the FO-HG system. The FO process-induced flux experiences a decrease when the hydrogel mass is reduced from 1.5 g to 0.5 g, as shown in Fig. 6a–c. This reduction in hydrogel mass during the FO process leads to a decrease in the overall swelling pressure, which is equal to the sum of the swelling pressures exerted by each individual hydrogel particle. In essence, the capacity to absorb water diminishes, leading to a decline in the overall driving force of the process and consequently reducing the flux.

The investigation on the impact of hydrogel particle size in the FO-HG system demonstrates that smaller hydrogel particles exhibit a higher flux in comparison to larger particles, as shown in Fig. 6d. Fig. 6e illustrates the particle size distribution of three hydrogel samples. The particles were classified into three groups according to their average size: 200, 400, and 550 μm. These groups were arranged in ascending order from smallest to largest, referred to as small, medium, and big respectively. It is noteworthy that as the particle size decreased, the sharpness of the distribution increased, resulting in a narrower particle size band.

The following interpretation can be illuminating regarding the observations. The reason for these effects, according to Omidian et al., is that small absorbents have more surface area per volume that are accessible to water than large absorbents. Additional water is accommodated by the interstitial volume through typical capillary action. When considering the two extremes of the hydrogel particle sizes, it is conceivable that water drainage is quite simple in cases of extremely wide bores, i.e. larger particles. More water is absorbed at a given depth of permeation into the absorbent particles, which results in an increase in the rate of absorption and water being held in the interstitial volume in the capillaries among the particles is the cause of the increased equilibrium absorption value [40].The others also reported the same observations [60]. According to the evidence, the particles' swelling process involves of water molecules diffusion into the polymer network, as well as the relaxation of the polymer chains, resulting in a rubbery polymer state (swollen) on the most outer surface of the hydrogel particles. The diffusion rate of hydrogel particles decreases as one moves from the outer layer (the rubbery shell) to the more rigid part (the inner core) that has no swelling, as shown in Fig. 9f. The smaller the rigid core, the faster the swelling process [61].

The water flux in the FO-HG process is significantly influenced by the size of the hydrogel particle, as stated by Li et al. Using PSA with an average size of 150 μm as the draw agent resulted in a flux of 57.4 % higher than that of PSA with an average size of 600 μm. The similar trend was also observed in the FO process using the other modified synthesized PSA in their work. They asserted that the reason could be due to the different contact area between the hydrogel-hydrogel particles and the particle-membrane. The surface to volume ratio of smaller particles is higher, which leads to a larger area of contact and a higher water absorbency and water flux [62]. At the start of water uptake, a hydrogels' swelling ratio is almost identical regardless of the particle size according to Razmjou et al. report. However, the point at which the accelerated swelling occurs, the particle size becomes influential. A higher swelling ratio is a result of smaller hydrogel particles. In order to investigate the impact of interstitial volume and particle-membrane contact on water flux in the FO process, they modified the hydrogel into disk shapes to decrease the interstitial volumes. The disc exhibited a considerably lower water flux compared to the powder. However, the addition of a small quantity of hydrogel powder beneath the disc resulted in a significant increase in flux. This experiment has demonstrated that the impact of the contact areas between the hydrogel particles and the membrane surface on the water flux is of greater importance compared to the interstitial volumes [41].

Hence, it can be inferred that the impact of hydrogel particle size on swelling processes and the ultimate swelling ratio is attributed to three factors: i) the interstitial volume of the particles, ii) the surface area of the particles per unit volume, and iii) the proper contact between the particle-particle and particles and the membrane surface. However, the mechanisms of the hydrogel swelling due to the change in the hydrogel particle size, for the tea-bag experiment can be meaningfully different from the FO-HG experiment. For the tea-bag experiment, the first two reasons can be involved, while for the FO-HG experiment, the two last reason are functioning. In the FO-HG experiment, the absence of free water (because of fast absorption of the permeated water across the membrane by the hydrogel) that can be transported through capillary action renders the interstitial volume insignificant. By reducing the size of the HG particles, the surface area of the particles increases. This, in turn, enhances the contact between particles, making it easier for water to be absorbed from the lower layers of the HG to the higher layers. Consequently, this results in greater swelling and flux. Furthermore, an optimal interaction between the particles and membrane surface significantly improves the initial absorption of water when the size of the HG particles decreases.

3.6. Investigating the swelling of hydrogel in un-constrained and constrained states

Fig. 7a, b and 7c display the swelling ratio outcomes of hydrogel in both constrained and un-constrained states when exposed to pure water along with the water flux using fabric and the FO membrane in the setup. The results indicated that the swelling in the un-constrained state was approximately two times greater than the swelling in the constrained state. The hydrogel particles have the capacity to absorb water from all directions in the un-constrained state as they are in contact with water in all sides. However, in the constrained state, the hydrogel was solely exposed to water from a single side (note Fig. 8). In essence, when hydrogel particles are in a constrained state, they can solely absorb

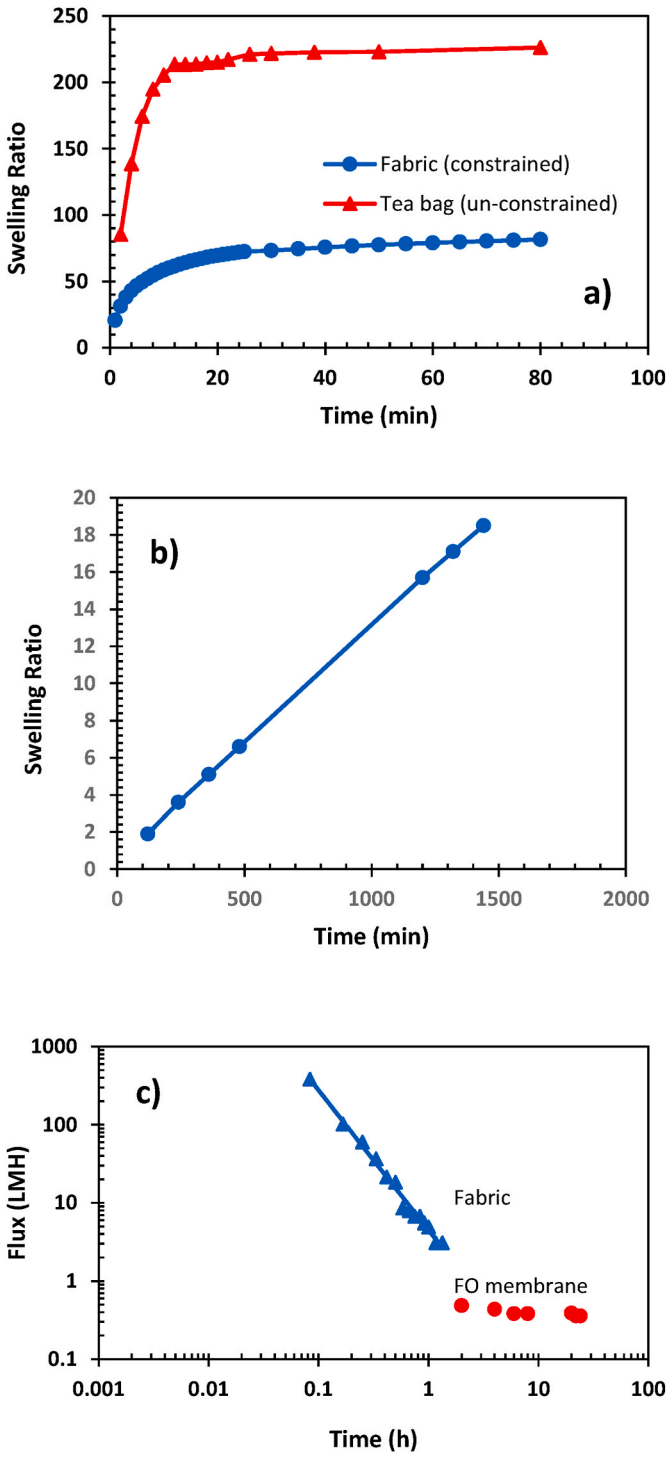

Fig. 7. a) hydrogel swelling ratio versus time for two constrained and un-constrained states, b) hydrogel swelling ratio in FO-HG system with membrane using pure water feed in FO-mode and c) comparison of water flux of FO-HG system constrained state with a piece of fabric and with membrane using pure water feed in FO-mode.

water from one side, specifically the surface of the membrane. Alternatively, water can permeate swollen hydrogel particles that are in close proximity to the membrane surface. Hence, the extent of water penetration in the constrained state, as mentioned previously, is influenced by factors such as the contact surface area between the membrane and the hydrogel, as well as the interaction among hydrogel particles. Therefore, when the contact surface between water and hydrogel particles is reduced, the absorption process takes place more gradually and the swelling decreases, resulting in a delay in reaching equilibrium absorption. Based on Fig. 7a, it is evident that the equilibrium swelling ratio in the constrained state has not been achieved even after approximately 80 min. Conversely, in the unconstrained state, the hydrogel has attained equilibrium swelling ratio (226) in a significantly shorter duration, less than 20 min. The water flux for the scenario involving a piece of fabric instead of the FO membrane is presented in Fig. 7c. The remarkable water flux achieved in this simple experiment effectively highlights the significance of the resistance offered by the existing FO membranes in a system employing HG as the draw agent, resulting in a reduction in the flux. In essence, the elimination of membrane resistance has led to a substantial increase in flux. Furthermore, apart from the significant increase in flux, there is also a substantial decrease in the time required to achieve equilibrium. This concern is evident when comparing the swelling of hydrogel in the FO setup using fabric (Fig. 7a) and membrane (Fig. 7b).

In other words, it can be stated that in the un-constrained state, when hydrogels are in contact with water from all directions, there is excess water in the space between hydrogel particles. This water is readily accessible and can be absorbed by the hydrogel. Hence, as the size of the hydrogel particles decreases, the particles surface area per volume increases, allowing for a greater amount of excess water to be absorbed. As a result, the process of diffusion and swelling takes place at an accelerated pace. Nevertheless, under constrained state and in the presence of the membrane (i.e. in the FO-HG system), as mentioned earlier, there is no excess water within the interstitial space of the hydrogel particles, and the water created by the osmotic pressure which passed through the membrane is immediately absorbed by the hydrogel.

4. Process suggestion and optimization

One important point that is very important in terms of the process is the low flux of fresh water by the FO-HG system. This issue can be resolved by the correct arrangement and operation of the process, overcoming the shortcomings discussed in the upper sections and as a result, the flux of the produced water can experience a significant improvement. The use of a high volume of hydrogel on the membrane and the implementation of the process in one stage does not result in success in fresh water with high flux. Complete saturation of the hydrogel to achieve equilibrium swelling is a time-consuming process that has a very slow logarithmic growth rate.

The final section of the article will focus on recommendations for addressing the low flux issue. One suggestion is to implement a process involving multiple cycles throughout the day and night (24 h), rather than a single step for water swelling and deswelling in a FO-HG system. Various stimuli can trigger the release of water from hydrogels, which varies according to the specific type of hydrogel. In this discussion, we have focused on a representative thermosensitive hydrogel of the lower critical solution temperature (LCST) type. The cyclic process profile of the heat-responsive FO-HG system is illustrated in Fig. 9. Fig. 9a displays the flux versus time profile, while Fig. 9b illustrates the temperature versus time profile. A full cycle encompasses the combination of the red curve (Cooling and swelling stage) and the green curve (Heating and deswelling stage). The entire cycle lasts from time A to E (Δt_{AE}). The red curve initiates with the cooling phase (Δt_{AB2}) and progresses to the swelling phase of the hydrogel (Δt_{B1C}). Point B1 marks the start of the swelling period. Similarly, the green curve commences with the heating phase (Δt_{CD2}) and completes with the water release phase (Δt_{D1E}).

Point D1 marks the initiation of the water release phase, representing a thermodynamic event. This point aligns with the LCST temperature. The phase of temperature elevation commences at the ambient temperature, progressing towards the LCST temperature, and continues beyond this point until reaching a specific optimal temperature (Δt_{CE}). Throughout a 24-h period, the time cycle of Δt_{AE}, which constitutes a complete process, is consistently repeated.

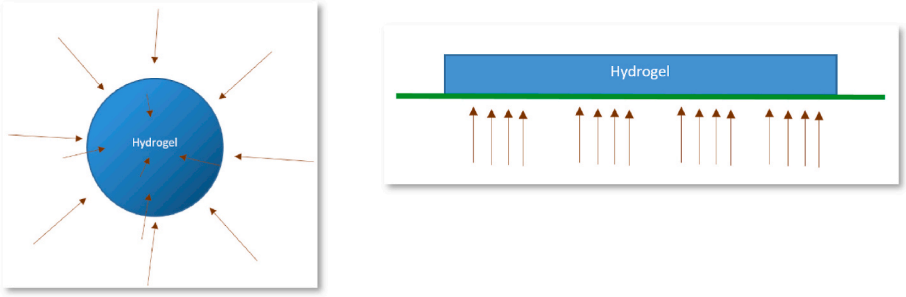

Fig. 8. Schematic of constrained versus un-constrained water absorption.

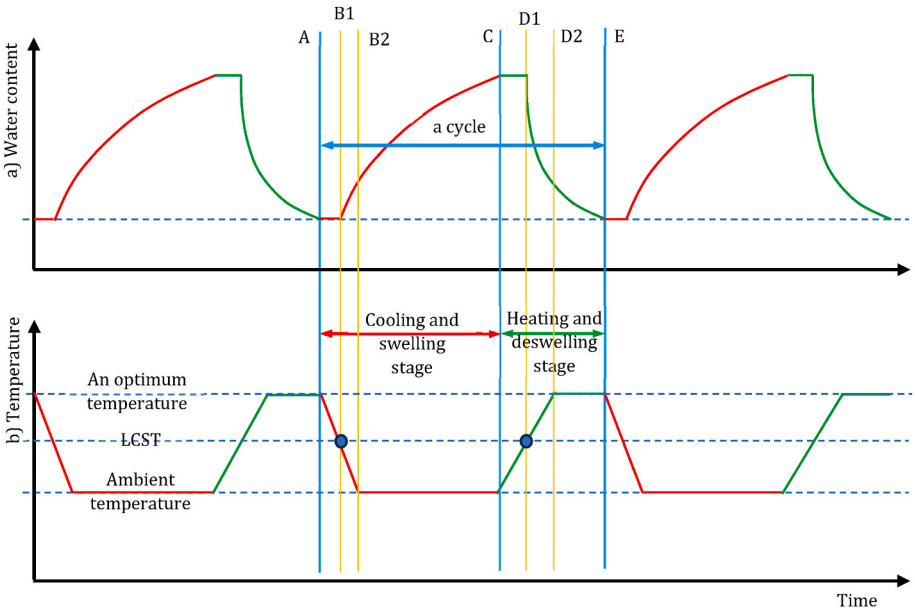

Fig. 9. Profile of the cyclic swelling-deswelling process for fresh water production via FO-HG system.

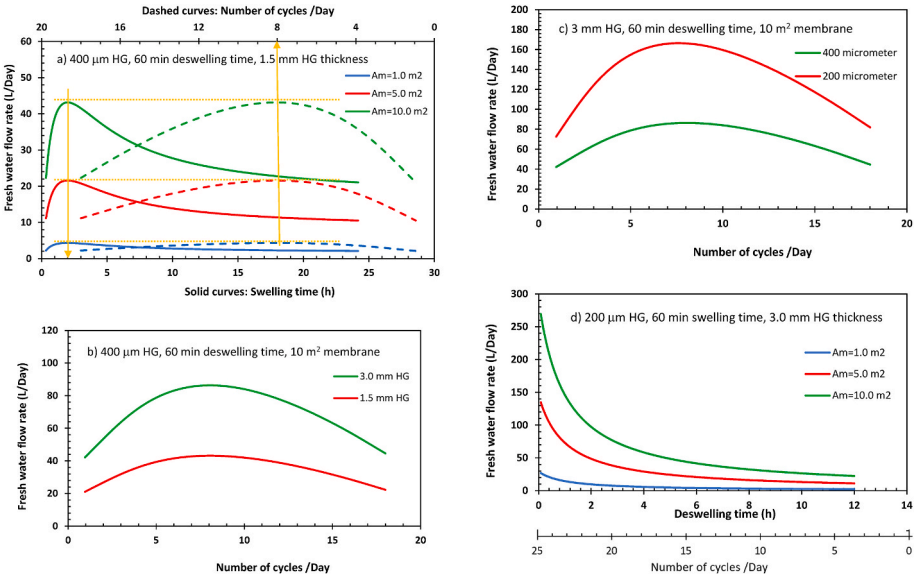

Fig. 10. Produced fresh water flow rate as a function of the number of cycles/Day, swelling or deswelling time for 30000 mg/L saltwater and PRO mode in a cyclic process; a) effect of membrane surface area, b) effect of HG thickness, c) effect of HG particle size and d) effect of deswelling time.

In this section, it is important to note that the laboratory data of sodium acrylate hydrogels has been utilized, with the assumption that these hydrogels exhibit thermos-responsive characteristics. Hence, this HG serves as a probe component. Consequently, the overall behavior and pattern of fresh water production rate variations are expected to be influenced by independent variables including hydrogel particle size, membrane surface area, thickness of hydrogel layer on the membrane surface, as well as the duration of swelling and deswelling in a single cycle, which will hold significant conceptual value.

The average flux for the medium and small hydrogel particles was derived using equations (A1) to (A7). For further information, please refer to appendix Figure S5a and S5b illustrate the variations of HG water flux over time for the two particle sizes tested for a feed of 30000 mg/L saltwater in PRO-mode. It is evident that the average flux is higher than the instantaneous flux.

Based on Fig. 10a–c, it can be observed that, in general, the amount of produced water reaches its maximum value with the increase of swelling time. This indicates that there is an optimal absorption time, corresponding to the number of cycles per day, to achieve the maximum amount of fresh water, as shown in Fig. 10a by orange arrows. The graph shows a steep slope from low times to optimal swelling time equal to ~2 h (optimal cycle number/day equal to ~8), reaching the maximum amount of produced water, while the slope is gentler from high absorption times to optimal absorption time. It is worth noting that the best swelling time (ideal number of cycles) is found within time periods less than 3 h. Moreover, as a rule, the quantity of fresh water also grows in line with the enlargement of the membrane surface.

The comparison of the curves in Fig. 10b reveals that the flux rises as the thickness of the hydrogel increases. This increase is nearly linear at lower thicknesses, but becomes non-linear at higher thicknesses, leading to a slower growth rate (not shown in the figures). The diffusion and absorption kinetics play a role in this phenomenon.

The fresh water yield from hydrogel particles with a size of 200 μm and a membrane surface area of 5 m^2 is nearly the same as the water yield from particles of 400 μm and a surface area of 10 m^2 (Fig. 10c). This indicates that selecting the optimal hydrogel particle size can result in significant economic savings and allow for a reduction in system dimensions, thereby directly impacting system operation from both a process and economic standpoint.

Fig. 10d reveals a noteworthy distinction: while the fresh the water flux exhibits a peak at an optimal swelling duration, the deswelling time graph lacks such an optimal point. Instead, the amount of fresh water produced is maximized at the minimum absorption time, which coincides with the highest number of cycles as shown in the figure. This observation highlights the fundamental difference between swelling and deswelling phenomena. Absorption or swelling is characterized as a kinetic process driven by the diffusion and uptake of water, whereas deswelling is identified as a thermodynamic process. As the duration of water release extends, the quantity of water produced diminishes. This conclusion is predicated on the premise that the release phenomenon is thermodynamic in nature; once specific conditions are met, such as those for a thermos-responsive hydrogel at or above the lower critical solution temperature (LCST), water is released with minimal resistance.

Attainment of thermodynamic conditions is crucial, as it determines when the discharge will occur rapidly. Consequently, as the discharge time decreases/increases, the number of process cycles increases/decreases throughout the day and night, resulting in a increases/decreases in the amount of produced water. It is worth noting that reducing the water release time, thereby increasing the number of cycles, leads to a notable variance in the maximum produced water with an increase in membrane surface area. Conversely, in longer release times or with a very low number of cycles, the amount of produced water remains constant and approaches each other asymptotically for various membrane surfaces.

5. Conclusion

This study investigated the behavior of an ionic hydrogel in the FO system, comparing it to salt water as a draw solution. When pure water was utilized as the feed, the swelling ratio in the un-constrained state was approximately 226, whereas in the constrained state, it reduced to half. However, when membrane was introduced into the FO setup, the swelling ratio experienced a significant decrease by one order of magnitude within the experimental timeframe. This decrease could be attributed to the membrane's high resistance. In the FO-HG and FO-NaCl systems, water flux is higher than salt solution feed when feed is pure water due to ECP and ICP. Water flux is higher in FO-NaCl compared to FO-HG in different modes with varying concentrations. FO-NaCl system generally has higher water flux than FO-HG. However, the FO-HG system maintains flux above zero at all feed concentrations up to 30000 mg/L. The hydrogel's ECP on the draw solution side is uncontrollable due to its immobility. Comparing FO-NaCl and FO-HG systems, the osmotic pressure difference between NaCl draw solution and pure water feed was greater than the swelling pressure between hydrogel and pure water. This led to higher water flux in FO-NaCl system, highlighting a drawback of FO-HG system. In some cases the FO-HG system, the osmotic pressure difference can exceed the osmotic pressure difference in the FO-NaCl system, leading to increased water flux. However, a perfect equivalence between an FO-NaCl system and an FO-HG system is extremely difficult to establish, considering the reasons stated. The limited contact area between the hydrogel and membrane reduces capillary force and water penetration, decreasing the flux. In the FO-HG system, the water flux in the PRO-mode was unexpectedly higher than in the FO-mode with salt water feed. This can be attributed to the counter-osmotic effect. Increasing the hydrogel quantity also increased water flux due to enhanced swelling pressure. Additionally, reducing hydrogel particle size resulted in enhanced flux, as seen in previous studies. Finally, the main emphasis was placed on suggestions for resolving the low flux issue. One recommendation put forward was the implementation of a process that involves multiple cycles throughout the day and night (24 h), as opposed to a single step for water swelling and deswelling in a FO-HG system. The discussion centered around a representative LCST hydrogel type. The study investigated the influence of hydrogel particle size, membrane surface, hydrogel layer thickness on the membrane surface, as well as swelling and deswelling time in a multicyclic process. While the swelling time displayed a peak at an optimal absorption duration, the deswelling time did not show a similar optimal point. This observation underscores the fundamental disparity between swelling and deswelling phenomena in terms of actual system operation.

Therefore, the exceptional capacity of hydrogel to have high absorption is not sufficient for success in desalination, and according to the findings of this research, the synthesis of a membrane with minimal resistance and therefore high flux and suitable selectivity is crucial. Ongoing work within our research group is dedicated to identifying a suitable membrane for the FO-HG application. Therefore, the design of the FO-HG system and understanding its challenges and how to solve them is very important and requires further studies.

CRediT authorship contribution statement

Seyed Abdollatif Hashemifard: Writing – review & editing, Writing – original draft, Supervision, Project administration, Formal analysis, Conceptualization. **Mohammad Ali Ghanavatyan:** Validation, Methodology, Formal analysis, Data curation. **Amir Jangizehi:** Writing – review & editing, Methodology, Investigation, Data curation. **Hasan Salehi:** Investigation, Formal analysis, Data curation. **Alireza Shakeri:** Writing – review & editing, Supervision, Conceptualization. **Qusay F. Alsalhy:** Writing – review & editing, Supervision, Conceptualization. **Dhiyaa Al-Timimi:** Validation, Methodology, Investigation, Formal analysis, Data curation. **Christoph Bantz:** Funding acquisition,

Conceptualization. **Michael Maskos:** Supervision, Funding acquisition, Conceptualization. **Sebastian Seiffert:** Writing – review & editing, Funding acquisition, Conceptualization, Supervision.

Declaration of Competing interest

The authors declare the following financial interests/personal relationships which may be considered as potential competing interests:

Sebastian Seiffert reports financial support was provided by Federal Ministry of Education and Research Bonn Office. If there are other authors, they declare that they have no known competing financial interests or personal relationships that could have appeared to influence the work reported in this paper.

Acknowledgements

This research was supported by the Sustainable Membrane Technology Research Group (SMTRG), Water Research Institute (WRI), Faculty of Petroleum, Gas and Petrochemical Engineering (FPGPE), Persian Gulf University, P.O. Box 75169-13798, Bushehr, Iran, and by the German Federal Ministry of Education and Research (BMBF) within the MEWAC program under project No. 02WME1613 (HydroDesal: Forward Osmosis Desalination by Thermo-Responsive Hydrogels for Small Villages Close to the Persian Gulf), Germany.

Appendix A. Supplementary data

Supplementary data to this article can be found online at https://doi.org/10.1016/j.memsci.2024.123408.

Appendix

The amount of fresh water for a specific thickness of hydrogel can be estimated by Equation (A1).

$$Q = \eta.\bar{J}_w.\Delta t_{cool+swel}.N.A_m \tag{A1}$$

where Q is produced fresh water (L/Day), $\bar{J}_w$ is average flux of absorbed water (LMH), $\Delta t_{\mathrm{cool}+swel}$ is cooling and swelling stage time ($\frac{h}{cycle}$), A_m is the membrane surface area (m^2) and N is the number of cycles per day $\left(\frac{number\ of\ cycles}{Day}\right)$ which is calculated as follows:

$$N = \frac{24}{\Delta t_{\mathrm{cool}+swel} + \Delta t_{\mathrm{heat}+\mathrm{des}wel}} \tag{A2}$$

where $\Delta t_{\mathrm{heat}+\mathrm{des}wel}$ is heating and deswelling stage time ($\frac{h}{cycle}$). It is established from equation (9)that there exists an inverse correlation between the number of cycles occurring within a day and night and the durations of water swelling and deswelling time. To accurately depict the true functionality of the HG in different scenarios, the efficiency coefficient, denoted as η, is introduced. It is highlighted that, when a fixed hydrogel thickness is assumed, the membrane surface area and the hydrogel quantity are linked and vary together. The average flux was obtained through equation (A3).

$$\bar{J}_w = \frac{1}{t - t_0}\int_{t_0}^{t} J_w(t)dt \tag{A3}$$

The instantaneous flux (LMH) change was approximated over time using exponential functions. These were presented with equations (A4) and (A5) for the HG medium size (400 μm) and HG small size (200 μm) respectively.

$$J_w = 0.13180 + 0.66856e^{-0.54336t} \tag{A4}$$

$$J_w = 0.193305 + 1.257887e^{-0.428167t} \tag{A5}$$

By substituting equations (A4) and (A5) into equation (A3), the average flux for the medium and small hydrogel particles was obtained through equations (A6) and (A7), respectively.

$$\bar{J}_w = \frac{1}{t}\left(1.23044 - 1.23044e^{-0.54336t} + 0.13180t\right) \tag{A6}$$

$$\bar{J}_w = \frac{1}{t}\left(2.93785 - 2.93785e^{-0.428167t} + 0.193305t\right) \tag{A7}$$

Data availability

Data will be made available on request.

References

[1] Z. Alihemati, S.A. Hashemifard, T. Matsuura, A.F. Ismail, N. Hilal, Current status and challenges of fabricating thin film composite forward osmosis membrane: a comprehensive roadmap, Desalination 491 (2020) 114557.

[2] L. Chekli, S. Phuntsho, H.K. Shon, S. Vigneswaran, J. Kandasamy, A. Chanan, A review of draw solutes in forward osmosis process and their use in modern applications, Desalination Water Treat. 43 (1–3) (2012) 167–184.

[3] W.J. Lim, B.S. Ooi, Applications of responsive hydrogel to enhance the water recovery via membrane distillation and forward osmosis: a review, Journal of Water Process Engineering 47 (2022) 102828.

[4] D.L. Shaffer, N.Y. Yip, J. Gilron, M. Elimelech, Seawater desalination for agriculture by integrated forward and reverse osmosis: improved product water quality for potentially less energy, J. Membr. Sci. 415–416 (2012) 1–8.

[5] K. Lutchmiah, A.R.D. Verliefde, K. Roest, L.C. Rietveld, E.R. Cornelissen, Forward osmosis for application in wastewater treatment: a review, Water Res. 58 (2014) 179–197.

[6] M.A. Shannon, P.W. Bohn, M. Elimelech, J.G. Georgiadis, B.J. Mariñas, A. M. Mayes, Science and technology for water purification in the coming decades, Nature 452 (7185) (2008) 301–310.

[7] G. Wade Miller, Integrated concepts in water reuse: managing global water needs, Desalination 187 (1) (2006/02/05/2006) 65–75.
[8] T. Arnot, D. Mattia, A review of reverse osmosis membrane materials for desalination–development to date and suture potential, J. Membr. Sci. 370 (2011) 1–22.
[9] J.O. Kessler, C.D. Moody, Drinking water from sea water by forward osmosis, Desalination 18 (3) (1976) 297–306.
[10] J.R. McCutcheon, M. Elimelech, Influence of concentrative and dilutive internal concentration polarization on flux behavior in forward osmosis, J. Membr. Sci. 284 (1) (2006) 237–247.
[11] C.D. Moody, J.O. Kessler, Forward osmosis extractors, Desalination 18 (3) (1976) 283–295.
[12] T.Y. Cath, A.E. Childress, M. Elimelech, Forward osmosis: principles, applications, and recent developments, J. Membr. Sci. 281 (1) (2006) 70–87.
[13] K.L. Hickenbottom, et al., Forward osmosis treatment of drilling mud and fracturing wastewater from oil and gas operations, Desalination 312 (2013) 60–66.
[14] W.A. Suwaileh, D.J. Johnson, S. Sarp, N. Hilal, Advances in forward osmosis membranes: altering the sub-layer structure via recent fabrication and chemical modification approaches, Desalination 436 (2018) 176–201.
[15] J. Wang, X. Liu, Forward osmosis technology for water treatment: recent advances and future perspectives, J. Clean. Prod. 280 (2021) 124354.
[16] Y.-N. Wang, K. Goh, X. Li, L. Setiawan, R. Wang, Membranes and processes for forward osmosis-based desalination: recent advances and future prospects, Desalination 434 (2018) 81–99.
[17] S. Zhao, L. Zou, C.Y. Tang, D. Mulcahy, Recent developments in forward osmosis: opportunities and challenges, J. Membr. Sci. 396 (2012) 1–21.
[18] S. Lee, C. Boo, M. Elimelech, S. Hong, Comparison of fouling behavior in forward osmosis (FO) and reverse osmosis (RO), J. Membr. Sci. 365 (1) (2010) 34–39.
[19] T.-S. Chung, S. Zhang, K.Y. Wang, J. Su, M.M. Ling, Forward osmosis processes: yesterday, today and tomorrow, Desalination 287 (2012) 78–81.
[20] Q. Ge, M. Ling, T.-S. Chung, Draw solutions for forward osmosis processes: developments, challenges, and prospects for the future, J. Membr. Sci. 442 (2013) 225–237.
[21] J. Su, S. Zhang, M.M. Ling, T.-S. Chung, Forward osmosis: an emerging technology for sustainable supply of clean water, Clean Technol. Environ. Policy 14 (2012) 507–511.
[22] W.F. Blatt, A. Dravid, A.S. Michaels, L. Nelsen, Solute polarization and cake formation in membrane ultrafiltration: causes, consequences, and control techniques, in: Membrane Science and Technology, Springer, 1970, pp. 47–97.
[23] A.S. Michaels, New separation technique for CPI, Chem. Eng. Prog. 64 (12) (1968) 31.
[24] M.C. Porter, Concentration polarization with membrane ultrafiltration, Ind. Eng. Chem. Prod. Res. Dev. 11 (3) (1972) 234–248.
[25] Q. Ge, J. Su, T.-S. Chung, G. Amy, Hydrophilic superparamagnetic nanoparticles: synthesis, characterization, and performance in forward osmosis processes, Ind. Eng. Chem. Res. 50 (1) (2011) 382–388.
[26] M.M. Ling, T.-S. Chung, X. Lu, Facile synthesis of thermosensitive magnetic nanoparticles as "smart" draw solutes in forward osmosis, Chem. Commun. 47 (38) (2011) 10788–10790, https://doi.org/10.1039/C1CC13944D.
[27] M.M. Ling, K.Y. Wang, T.-S. Chung, Highly water-soluble magnetic nanoparticles as novel draw solutes in forward osmosis for water reuse, Ind. Eng. Chem. Res. 49 (12) (2010) 5869–5876.
[28] D. Li, X. Zhang, J. Yao, Y. Zeng, G.P. Simon, H. Wang, Composite polymer hydrogels as draw agents in forward osmosis and solar dewatering, Soft Matter 7 (21) (2011) 10048–10056, https://doi.org/10.1039/C1SM06043K.
[29] A. Razmjou, M.R. Barati, G.P. Simon, K. Suzuki, H. Wang, Fast deswelling of nanocomposite polymer hydrogels via magnetic field-induced heating for emerging FO desalination, Environmental Science & Technology 47 (12) (2013) 6297–6305.
[30] Q. Chai, Y. Jiao, X. Yu, Gels 3 (1) (2017) 6.
[31] M.M. Elsayed, Hydrogel preparation technologies: relevance kinetics, thermodynamics and scaling up aspects, J. Polym. Environ. 27 (4) (2019) 871–891.
[32] S. Gulrez, Saphwan Al-assaf, O. Phillips Glyn, Hydrogels: methods of preparation, characterisation and applications, Advanced Research 6 (2) (2003) 105–121.
[33] W.M. Kulicke, H. Nottelmann, Structure and swelling of some synthetic, semisynthetic, and biopolymer hydrogels, Polymers in Aqueous Media 223 (1989) 15–44. Advances in Chemistry, no. 223): American Chemical Society.
[34] V. Sinha, S. Chakma, Advances in the preparation of hydrogel for wastewater treatment: a concise review, J. Environ. Chem. Eng. 7 (5) (2019) 103295.
[35] F. Ullah, M.B.H. Othman, F. Javed, Z. Ahmad, H.M. Akil, Classification, processing and application of hydrogels: a review, Mater. Sci. Eng. C 57 (2015) 414–433.
[36] D. Li, X. Zhang, J. Yao, G.P. Simon, H. Wang, Stimuli-responsive polymer hydrogels as a new class of draw agent for forward osmosis desalination, Chem. Commun. 47 (6) (2011) 1710–1712, https://doi.org/10.1039/C0CC04701E.
[37] J. Wei, C. Qiu, C.Y. Tang, R. Wang, A.G. Fane, Synthesis and characterization of flat-sheet thin film composite forward osmosis membranes, J. Membr. Sci. 372 (1) (2011) 292–302.
[38] M. Qasim, F.W. Khudhur, A. Aidan, N.A. Darwish, Ultrasound-assisted forward osmosis desalination using inorganic draw solutes, Ultrason. Sonochem. 61 (2020) 104810.
[39] R.W. Holloway, R. Maltos, J. Vanneste, T.Y. Cath, Mixed draw solutions for improved forward osmosis performance, J. Membr. Sci. 491 (2015) 121–131.
[40] H. Omidian, S.A. Hashemi, P.G. Sammes, I. Meldrum, Modified acrylic-based superabsorbent polymers (dependence on particle size and salinity), Polymer 40 (7) (1999) 1753–1761.
[41] A. Razmjou, G.P. Simon, H. Wang, Effect of particle size on the performance of forward osmosis desalination by stimuli-responsive polymer hydrogels as a draw agent, Chem. Eng. J. 215–216 (2013) 913–920.
[42] Y. Cai, X.M. Hu, A critical review on draw solutes development for forward osmosis, Desalination 391 (2016) 16–29.
[43] S. Ma, X. Wu, L. Fan, Q. Wang, Y. Hu, Z. Xie, Effect of different draw solutions on concentration polarization in a forward osmosis process: theoretical modeling and experimental validation, Ind. Eng. Chem. Res. 62 (8) (2023) 3672–3683.
[44] Y. Wang, M. Zhang, Y. Liu, Q. Xiao, S. Xu, Quantitative evaluation of concentration polarization under different operating conditions for forward osmosis process, Desalination 398 (2016) 106–113.
[45] L.E. Bromberg, E.S. Ron, Temperature-responsive gels and thermogelling polymer matrices for protein and peptide delivery, Adv. Drug Deliv. Rev. 31 (3) (1998) 197–221.
[46] T.-S. Chung, X. Li, R.C. Ong, Q. Ge, H. Wang, G. Han, Emerging forward osmosis (FO) technologies and challenges ahead for clean water and clean energy applications, Current Opinion in Chemical Engineering 1 (3) (2012) 246–257.
[47] K. Zhang, F. Li, Y. Wu, L. Feng, L. Zhang, Construction of ionic thermo-responsive PNIPAM/γ-PGA/PEG hydrogel as a draw agent for enhanced forward-osmosis desalination, Desalination 495 (2020) 114667.
[48] A. Shakeri, H. Salehi, M. Taghvay Nakhjiri, E. Shakeri, N. Khankeshipour, F. Ghorbani, Carboxymethylcellulose-quaternary graphene oxide nanocomposite polymer hydrogel as a biodegradable draw agent for osmotic water treatment process, Cellulose 26 (3) (2019) 1841–1853.
[49] Y. Hartanto, S. Yun, B. Jin, S. Dai, Functionalized thermo-responsive microgels for high performance forward osmosis desalination, Water Res. 70 (2015) 385–393.
[50] W.-F. Lee, G.-H. Lin, Superabsorbent polymeric materials VIII: swelling behavior of crosslinked poly[sodium acrylate-co-trimethyl methacryloyloxyethyl ammonium iodide] in aqueous salt solutions, J. Appl. Polym. Sci. 79 (9) (2001) 1665–1674.
[51] X. Wang, et al., Molecular dynamics simulation of the surface tension of aqueous sodium chloride: from dilute to highly supersaturated solutions and molten salt, Atmos. Chem. Phys. 18 (23) (2018) 17077–17086.
[52] A. Tiraferri, N.Y. Yip, W.A. Phillip, J.D. Schiffman, M. Elimelech, Relating performance of thin-film composite forward osmosis membranes to support layer formation and structure, J. Membr. Sci. 367 (1) (2011) 340–352.
[53] L. Zhao, Z. Liu, F. Soyekwo, C. Liu, Y. Hu, Q.J. Niu, Exploring the feasibility of novel double-skinned forward osmosis membranes with higher flux and superior anti-fouling properties for sludge thickening, Desalination 523 (2022) 115410.
[54] M. Eyvaz, S. Arslan, D. İmer, E. Yüksel, İ. Koyuncu, Development, C. Status. Forward Osmosis Membranes–A Review: Part I, 2018, pp. 11–40.
[55] A.J. Ansari, F.I. Hai, W.E. Price, J.E. Drewes, L.D. Nghiem, Forward osmosis as a platform for resource recovery from municipal wastewater - a critical assessment of the literature, J. Membr. Sci. 529 (2017) 195–206.
[56] S. Zhao, Osmotic pressure versus swelling pressure: comment on "bifunctional polymer hydrogel layers as forward osmosis draw agents for continuous production of fresh water using solar energy", Environmental Science & Technology 48 (7) (2014) 4212–4213.
[57] H. Wang, J. Wei, G.P. Simon, Response to osmotic pressure versus swelling pressure: comment on "bifunctional polymer hydrogel layers as forward osmosis draw agents for continuous production of fresh water using solar energy", Environmental Science & Technology 48 (7) (2014) 4214–4215.
[58] P.J. Flory, Principles of Polymer Chemistry, Cornell university press, 1953.
[59] R. Ou, H. Zhang, G.P. Simon, H. Wang, Microfiber-polymer hydrogel monolith as forward osmosis draw agent, J. Membr. Sci. 510 (2016) 426–436.
[60] S. Kiatkamjornwong, K. Mongkolsawat, M. Sonsuk, Synthesis and property characterization of cassava starch grafted poly[acrylamide-co-(maleic acid)] superabsorbent via γ-irradiation, Polymer 43 (14) (2002) 3915–3924.
[61] G. Gerlach, KF. Arndt, Hydrogel Sensors and Actuators. Chapter Hydrogels for Chemical Sensors 6, Springer. Springer, 2010.
[62] D. Li, X. Zhang, G.P. Simon, H. Wang, Forward osmosis desalination using polymer hydrogels as a draw agent: influence of draw agent, feed solution and membrane on process performance, Water Res. 47 (1) (2013) 209–215.